Aalborg Universitet

AALBORG UNIVERSITY

Interharmonics from Grid-Connected PV Systems

Mechanism and Mitigation

Sangwongwanich, Ariya; Yang, Yongheng; Sera, Dezso; Blaabjerg, Frede

Interharmonics from Grid-Connected PV Systems: Mechanism and Mitigation

Ariya Sangwongwanich[1], *IEEE Student Member*, Yongheng Yang[2], *IEEE Member*,
Dezso Sera[3], *IEEE Member*, and Frede Blaabjerg[4], *IEEE Fellow*

Department of Energy Technology
Aalborg University
Pontoppidanstraede 111, Aalborg DK-9220, Denmark
ars@et.aau.dk[1], yoy@et.aau.dk[2], des@et.aau.dk[3], fbl@et.aau.dk[4]

Abstract—As the penetration level of grid-connected Photovoltaic (PV) systems increases, the power quality is one of the major concerns for system operators and the demands are becoming even stricter. The impact of interharmonics on the grid has been acknowledged in recent research when considering a large-scale adoption of PV inverters. However, the origins of interharmonics remain unclear. Thus, this paper performs tests on a commercial PV inverter to explore interharmonic generation and more important investigates the mechanism of interharmonic emission. The investigation reveals that the perturbation of the Maximum Power Point Tracking (MPPT) algorithm is one of the sources that induce interharmonics in the grid current, especially at low-power operating conditions. Accordingly, three mitigation solutions are discussed to address this issue, and simulations have been carried out to verify the effectiveness of the solutions. Simulation results indicate that the constant-voltage MPPT method is the most suitable solution to the mitigation of interharmonics introduced by the MPPT operation, as it avoids the perturbation in the PV voltage during operation.

Index Terms—Photovoltaic (PV) systems, inverters, maximum power point tracking (MPPT), interharmonics, power quality.

I. INTRODUCTION

Power quality is one of the major concerns along with the fast growing installation of grid-connected PV systems [1]–[3]. It is reported that PV inverters might be one source of harmonics and/or interharmonics that are delivered to the grid, challenging the power quality of the utility networks [4]–[9]. Recent studies have revealed that a large-scale adoption of grid-connected PV inverters may be one contributor to the increasing interharmonics appearing in the grid currents, causing voltage fluctuations and light flicker [10]–[16]. As the high penetration level of PV systems is still growing, the impact of interharmonics may become higher and worsen the power quality. Moreover, it has been observed in previous research that the interharmonic issue is pronounced at the low-power operations [13]–[16], where some PV inverters are disconnected for protection [12]. However, disconnecting PV inverters will lead to considerable energy losses, which should be avoided. Therefore, the interharmonic issues of the PV inverter at low-power operations should be explored in order to design proper mitigation solutions.

In general, there might be several sources of interharmonics in power electronic systems [17]: two asynchronous conver-
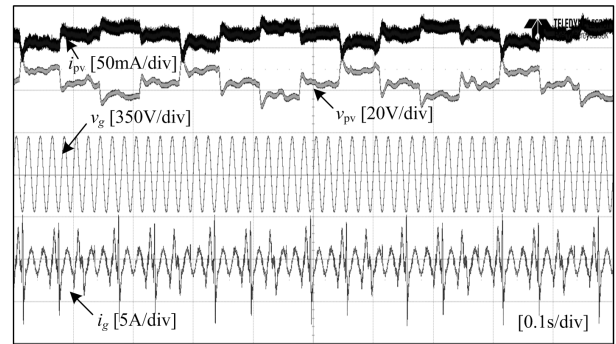

Fig. 1. Experimental results from a commercial 15-kW PV inverter operating at 2 % of the rated power (i.e., MPPT operation), where v_{pv} is the PV voltage, i_{pv} is the PV current, v_g is the grid voltage, and i_g is the grid current.

sion systems (ac-dc-ac) like in motor drives [18]–[20], time-varying loads like arc furnaces [21], mechanical vibrations like in wind turbines [22]. However, in the case of PV inverters, one potential root-cause of interharmonics may be related to the Maximum Power Point Tracking (MPPT) control [13]–[15]. This has been observed experimentally with commercial PV inverters [13]–[16], where a considerable amount of interharmonics from PV inverters have been measured at low-power operations. Specifically, it is suggested in [13]–[15] that the interharmonic frequency spectrum correlates with the MPPT frequency. Similar characteristic has also been observed in a PV inverter from a leading manufacturer tested at Aalborg University. The test results in Fig. 1 and the frequency spectrum analysis in Fig. 2 demonstrate the existence of interharmonics, at least at low-power conditions. Nevertheless, it is very difficult to obtain the designed controller parameters of commercial PV inverters under test. Thus, mapping the interharmonic frequency to the MPPT or other control frequencies is not possible. That is, the mechanism of the interharmonic emission is not yet fully understood, and the above analysis is done from observations of measurements. As a consequence, solutions to mitigating interharmonics have not been discussed so far either.

In light of the above issues, a more in-depth analysis of the interharmonic emission from grid-connected PV inverters
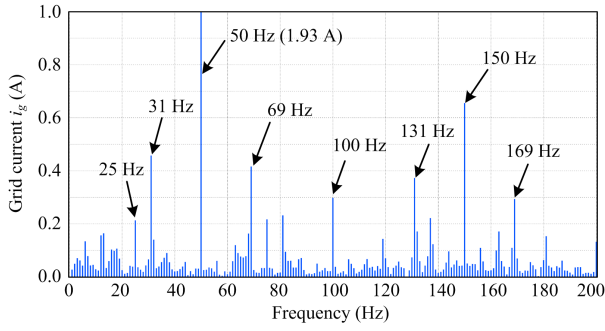
Fig. 2. Frequency spectrum of the grid current from the measurements shown in Fig. 1 with the frequency resolution of 1 Hz.

is necessary. Hence, this paper explores the mechanism of interharmonic emission from PV inverters in § II, where it has been observed that the perturbation of the MPPT operation is the main cause of interharmonics in the grid current. More important, solutions to the mitigation of interharmonics are discussed in § III. Simulations on a 3-kW single-phase PV inverter have been carried out in § IV, in order to verify the analysis and the effectiveness of the interharmonic mitigation solutions. Finally, concluding remarks are given in § V.

II. INTERHARMONICS IN GRID-CONNECTED PV INVERTERS

A. Single-Phase Grid-Connected PV Inverters

A typical system configuration of single-phase single-stage grid-connected PV systems is shown in Fig. 3. It consists of three parts: PV panels (or arrays), PV inverters (with output LCL-filters), and the ac grid. The PV inverters (e.g., full-bridge inverter) play a major role in controlling the power delivery from the PV arrays to the ac grid. The typical control structure of single-phase single-stage grid-connected PV inverters is shown in Fig. 3 [23], and the system parameters are given in Table I. In order to ensure a maximum power extraction from the PV arrays, an MPPT algorithm (e.g., Perturb and Observe - P&O) is employed to determine the reference dc-link voltage v_{dc}^* (i.e., PV voltage) during operation. Then, the dc-link voltage controller, which is based on a Proportional Integral (PI) controller, regulates the dc-link voltage v_{dc} accordingly through the control of the grid current i_g. For single-phase systems, the dc-link voltage v_{dc} contains double-line frequency components (e.g., 100 Hz), due to the power coupling between the PV side (dc power) and the single-phase grid (ac power). Thus, a Low-Pass Filter (LPF) can be used to improve the dc-link voltage control performance [24]. Notably, a Phase-Locked Loop (PLL) is also required for synchronization of the grid current with the grid voltage, as shown in Fig. 3.

B. Interharmonic Characteristic of PV Inverters

It has been reported in [16] that PV inverters have a so-called "power-dependent" interharmonic (and also harmonic) characteristic, where the emission level increases at the low-power operation. In order to demonstrate this, two simulation
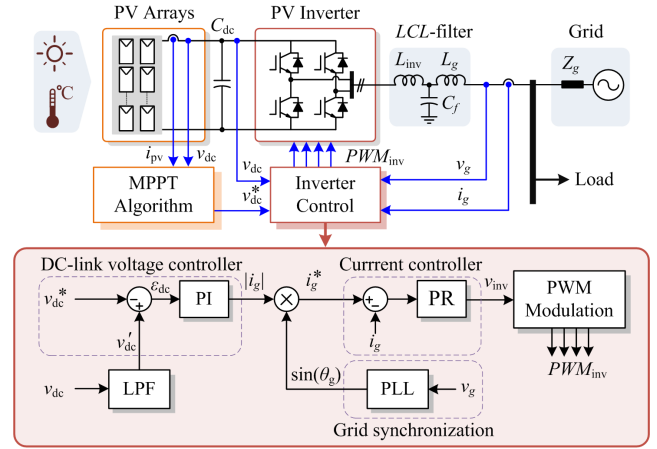

Fig. 3. System configuration and control structure of single-phase grid-connected PV systems with MPPT operation (PI - Proportional Integral, PR - Proportional Resonant, PWM - Pulse Width Modulation).

TABLE I
PARAMETERS OF THE SINGLE-PHASE GRID-CONNECTED PV SYSTEM.

PV rated power	3 kW
DC-link capacitor	C_{dc} = 1100 μF
LCL-filter	L_{inv} = 4.8 mH, L_g = 2 mH, C_f = 4.3 μF
Switching frequency	Full-Bridge inverter: f_{inv} = 8 kHz
Controller sampling frequency	f_s = 20 kHz
DC-link voltage	v_{dc}^* = 450 V
Grid nominal voltage (RMS)	V_g = 230 V
Grid nominal frequency	ω_0 = 2π×50 rad/s
MPPT algorithm sampling rate	f_{MPPT} = 20 Hz
MPPT perturbation step size	v_{step} = 4 V

cases with the system parameters in Table I have been carried out. Results are shown in Figs. 4 and 5, where the PV inverter operates at 100 % and 5 % of the rated power, respectively. In both cases, the MPPT operation is stable and the dc-link voltage (PV voltage) oscillates around three optimum operating points with the MPPT algorithm sampling frequency f_{MPPT} of 20 Hz, as it is shown in Fig. 4. This is considered as the optimum MPPT operation in [25] and similar behaviors have been observed in the commercial PV inverter as shown in Fig. 1. However, the corresponding injected grid current is much more distorted at the low-power operation, as it is shown in Fig. 5(b). The frequency spectrum of the grid current (with the frequency resolution of 1 Hz) in Fig. 6(a) shows that the interharmonic level is higher (in absolute value) when the PV inverter operates at 5 % of the rated power, even though the fundamental component of the grid current (i.e., 50 Hz) is much less than that at the rated power. In that case, the interharmonic emission from the PV inverter is significant.

C. Interharmonic Emission Mechanism

It is necessary to understand the root causes of interharmonics in order to design a proper mitigation solution. From the results in Fig. 5(b), it can be noticed that the grid current is significantly distorted during the dc-link voltage change
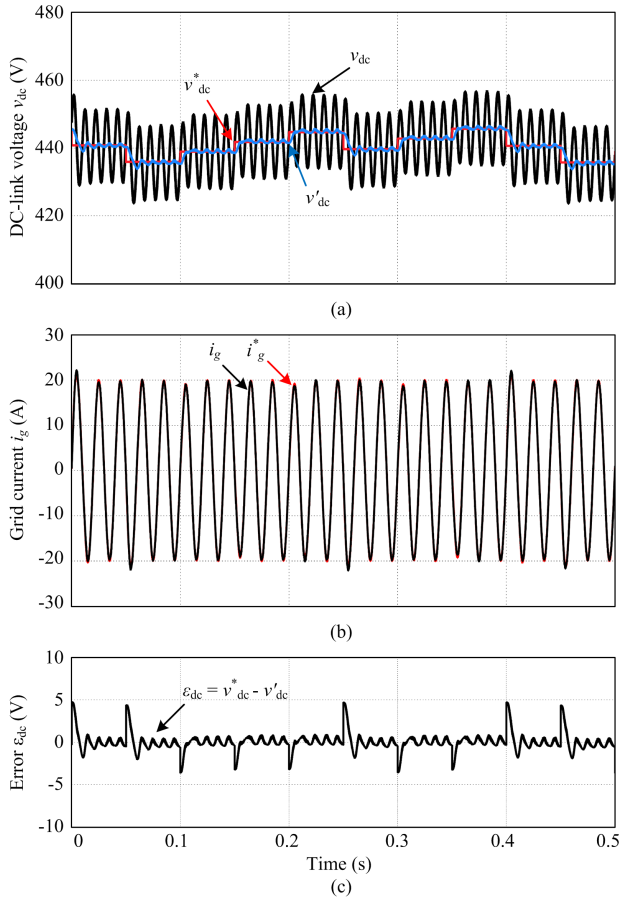
Fig. 4. Simulation results of the PV inverter operated at 100 % of the rated power (i.e., 3 kW) at the steady-state MPPT operation: (a) dc-link voltage (v_{dc}^* is the reference dc-link voltage, v_{dc} is the measured dc-link voltage, v_{dc}' is the dc component of v_{dc}), (b) grid current (i_g^* is the reference grid current, i_g is the measured grid current), and (c) error in the dc-link voltage ε_{dc}.
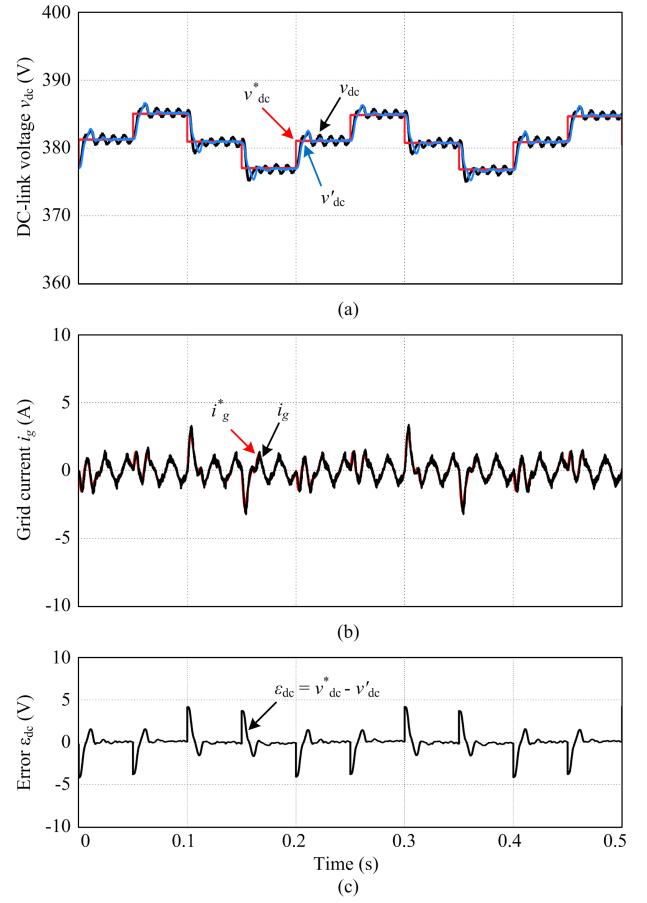
Fig. 5. Simulation results of the PV inverter operated at 5 % of the rated power (i.e., 0.15 kW) at the steady-state MPPT operation: (a) dc-link voltage (v_{dc}^* is the reference dc-link voltage, v_{dc} is the measured dc-link voltage, v_{dc}' is the dc component of v_{dc}), (b) grid current (i_g^* is the reference grid current, i_g is the measured grid current), and (c) error in the dc-link voltage ε_{dc}.

(i.e., during the MPPT perturbation). In fact, at the beginning of each MPPT period, the MPPT algorithm will introduce a step change in the dc-link voltage reference with an amplitude corresponding to the perturbation step-size of the MPPT algorithm, i.e., v_{step}. This will result in an error (ε_{dc}) at the input of the dc-link voltage controller during transients as shown in Fig. 5(c). Due to the periodical MPPT perturbation, the error in the dc-link voltage ε_{dc} is typically a periodic waveform, which contains a certain set of frequency components f_n. Since the dc-link voltage controller is the outer control loop of the current controller (Fig. 3), the frequency components of the dc-link voltage error ε_{dc} can propagate to the grid current amplitude $|i_g|$. Then, the multiplication between the grid current amplitude $|i_g|$ and the phase angle of the grid voltage (i.e., $\sin\theta_g$) will cause the amplitude modulation between the two signals, resulting in the reference grid current i_g^* with the frequency components of $f_n \pm f_g$, where f_g is the grid frequency. As a consequence, the current i_g injected to the grid may contain interharmonic components due to the amplitude modulation with the frequency components of $f_n \pm f_g$ Hz.

The above analysis can be verified by considering the fre-

quency spectrum analysis of the error in the dc-link voltage in Fig. 6(b). It can be seen from the results that the interharmonic components are of $f_n = (2n-1)f_{MPPT}/4$ Hz, where f_{MPPT} is the MPPT algorithm sampling frequency and n is an integer number (e.g., $f_n = 5, 15, 25,...$ Hz for $f_{MPPT} = 20$ Hz). The dominant frequency components with high amplitudes are around 45, 55, and 65 Hz. If the grid voltage only contains the fundamental component (e.g., $f_g = 50$ Hz), which is the case in this simulation, the dominant frequencies after the frequency modulation should be 5, 15, 95, 105, and 115 Hz. This is in a close agreement with the frequency spectrum of the grid current shown in Fig. 6(a). Thus, the above frequency spectrum analysis shows that the main cause of interharmonics in the grid current is the transient response in the dc-link voltage controller during the MPPT perturbation.

III. MITIGATION OF INTERHAMONICS

According to the previous discussion, the grid current is distorted by the perturbation in the dc-link voltage (PV voltage) due to the MPPT algorithm. Normally, the MPPT algorithm will introduce a step-change in the reference dc-link
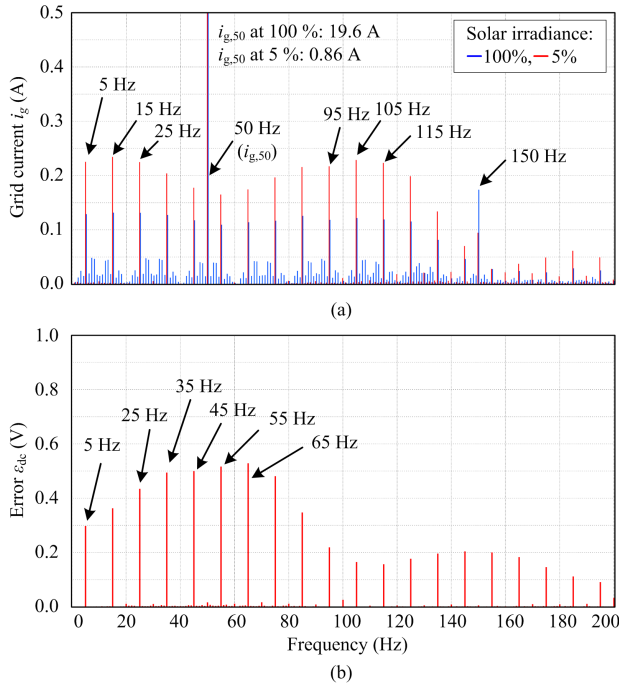
(a)

(b)

Fig. 6. Frequency spectrum analysis of the PV inverter during the steady-state MPPT operation: (a) grid current i_g in Figs. 4 and 5 and (b) error in the dc-link voltage ε_{dc} in Fig. 5 with the frequency resolution of 1 Hz. Fundamental component (50 Hz) of the gird current is: 19.6 A at 100 % of the rated power and 0.86 A at 5 % of the rated power.

voltage at the beginning of each MPPT period. This leads to a relatively aggressive transient behavior of the dc-link voltage controller, which will cause interharmonics (e.g., at the low-power operation), as it can be seen previously. In order to alleviate the above problem, this section presents three possible solutions to mitigate the interharmonics.

A. Adaptive Gain for the DC-link Voltage Controller

As it has been discussed previously, one of the sources of interharmonics in the grid current is the transient response of the dc-link voltage controller, which reacts relatively fast to changes in the reference dc-link voltage due to the MPPT perturbation. Therefore, reducing the proportional gain of the PI controller k_p, which affects the transient response of the controller, can decrease the abrupt change in the grid current and thereby effectively alleviate this problem. However, this will increase the settling time of the dc-link voltage controller, which may limit the perturbation rate of the MPPT algorithm. Notably, the maximum MPPT sampling rate is determined by the settling time of the dc-link voltage controller, as the dc-link voltage should reach its steady-state value before the next perturbation (from the MPPT algorithm) occurs. Thus, a possibility to avoid slow response time is to employ an adaptive gain for the PI controller, where the proportional gain k_p should be adjusted as a function of the PV power P_{pv}, as it is shown in Fig. 7. In this way, a small k_p will be used for low-power operations and the interharmonic level is reduced, while the controller dynamic is maintained at high-power operations.
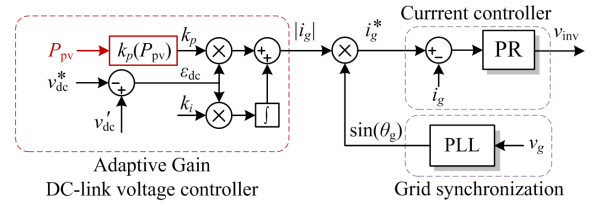

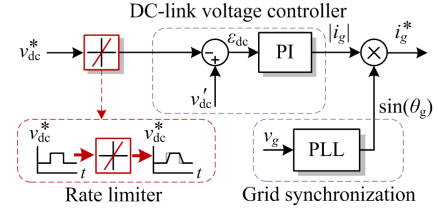Fig. 7. Control structure of the PV inverter using an adaptive gain for the dc-link voltage controller.

Fig. 8. Control structure of the PV inverter using a rate limiter for the dc-link voltage controller.

B. Rate Limiter for the DC-link Voltage Controller

Alternatively, a smooth change in the dc-link voltage at each MPPT perturbation can also be achieved by directly limiting the change rate of the reference dc-link voltage. In this approach, the reference dc-link voltage is changed from the previous value to the new set-point with a ramp-changing manner. This is achieved by using a rate limiter to limit the change rate of the reference dc-link voltage, as it is shown in Fig. 8. In this case, the control parameters of the dc-link voltage controller remain unchanged. This will result in a smooth transition during transients of each MPPT period, where the overshoot in the dc-link voltage during transients is minimized (as it will be shown in Fig. 9(b)).

It is worth mentioning that limiting the change rate in the reference dc-link voltage will not worsen the MPPT efficiency, as the main contributor to the PV power losses is the power oscillation in the steady-state MPPT operation. That is affected by the perturbation step-size of the MPPT algorithm [25]. The objective of the dc-link voltage controller is only to ensure that the operating point of the PV system (e.g., PV voltage) is regulated according to the set-point given by the MPPT algorithm, where an extremely fast dynamic response is not necessary. The only constraint for the rate limiter is that the reference dc-link voltage has to change from the previous value to the new set-point within one MPPT sampling period in order to ensure that the dc-link voltage reach its steady-state value before the next MPPT perturbation.

C. Constant-Voltage MPPT Method

In order to eliminate the interharmonics from the PV inverter, the perturbation of the dc-link voltage should be avoided at the low-power condition. This can be achieved by using a Constant-Voltage MPPT algorithm (CV-MPPT), where a constant reference dc-link voltage (PV voltage) is assigned
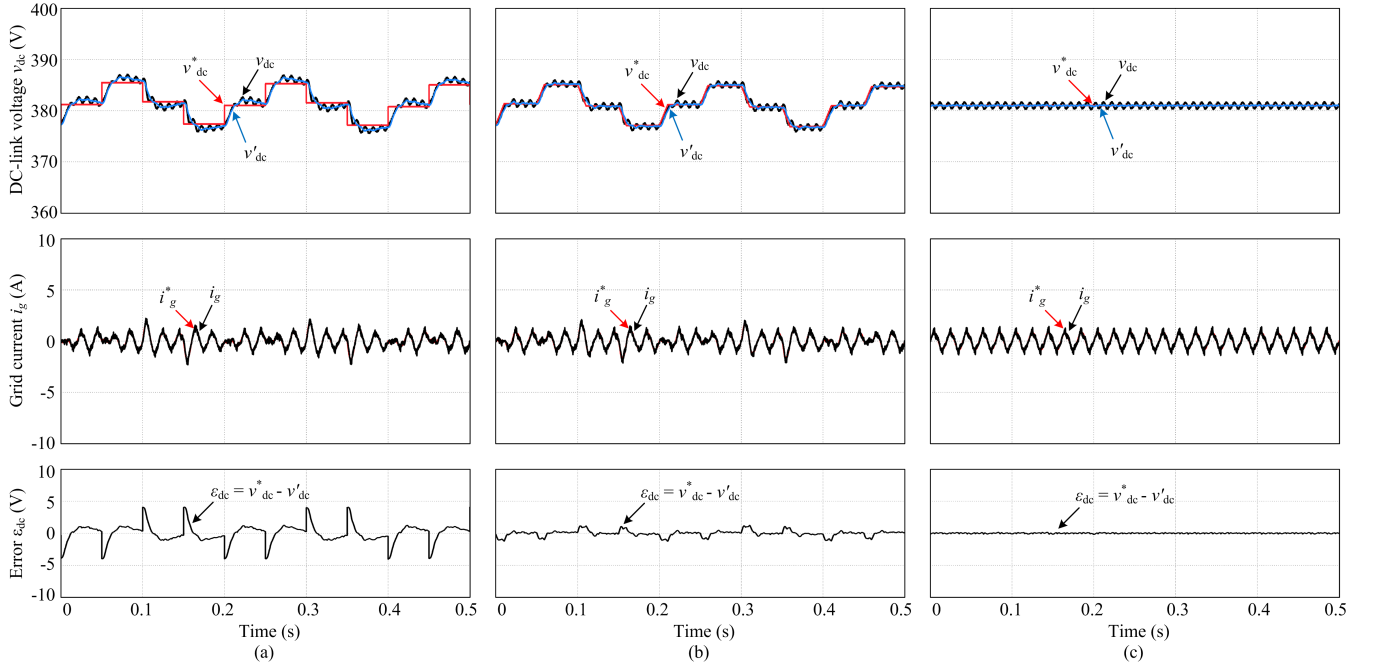
Fig. 9. Simulation results of the PV inverter operated at 5 % of the rated power (i.e., 0.15 kW) at the steady-state MPPT operation with the proposed mitigation solutions: (a) using an adaptive gain, (b) using a rate limiter, and (c) using a constant-voltage MPPT method, where v_{dc}^* is the reference dc-link voltage, v_{dc} is the measured dc-link voltage, v_{dc}' is the dc component of v_{dc}, i_g^* is the reference grid current, i_g is the measured grid current, ε_{dc} is the error in the dc-link voltage.

to the dc-link voltage controller without perturbations. The reference voltage is approximated as 71-78 % of the open-circuit voltage of the PV arrays [26]. Since the dc-link voltage (PV voltage) remains unchanged, there is no interaction between the dc-link voltage controller and the current controller, and thus the interharmonics due to the MPPT perturbation can be avoided. The shortcoming of this approach is the decrease in the MPPT accuracy, which leads to loss in the PV energy yield. Specifically, the variations in PV voltage at the MPP can be introduced due to the ambient temperature as well as solar irradiance level change. Therefore, the CV-MPPT algorithm should be activated only when the PV inverter operates at low-power conditions [27]. Otherwise, the P&O MPPT algorithm should be continuously employed.

IV. RESULTS AND DISCUSSION

Simulations of the three discussed solutions are carried out on the single-phase PV system in Fig. 3 with the system parameters given in Table I. The PV inverter operates under constant solar irradiance (i.e., steady-state MPPT) corresponding to 5 % of the rated power (i.e., 0.15 kW), where the interharmonics emission is pronounced. The performances of the three mitigation solutions under this operating condition are presented in Fig. 9. The frequency spectrum of the grid currents (in Fig. 9) is shown in Fig. 10, where it can be seen that all three methods can effectively reduce the interharmonic components in the grid current, compared to the case with the normal MPPT operation. Employing an adaptive gain and a rate limiter result in a similar grid current waveform,
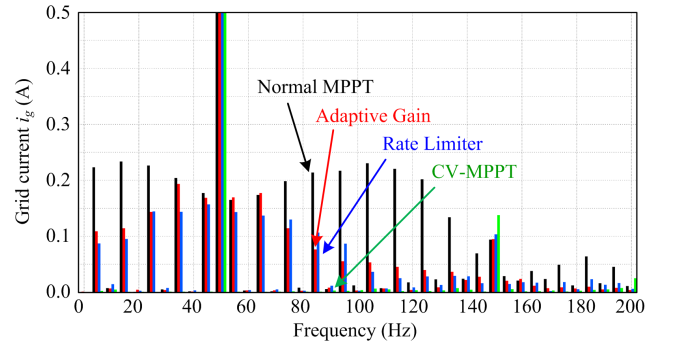

Fig. 10. Frequency spectrum of the PV inverter output current at the MPPT operation at 5 % of the rated power with the proposed mitigation solutions.

where an abrupt change in the grid current during the MPPT perturbation is significantly reduced (see Fig. 9), compared to the case in Fig. 5(b). As a consequence, the interharmonic level is significantly reduced, especially in the frequency range between 80-140 Hz, as it can be seen from the frequency spectrum in Fig. 10. Nevertheless, the CV-MPPT method is the most effective method among the three solutions in terms of minimizing the interharmonics. This is due to the fact that there is no perturbation in the case of CV-MPPT method, where the reference dc-link voltage is constant during the operation. However, the MPPT accuracy is compromised, as the reference dc-link voltage at the MPP is an approximation, which is a disadvantage of this method. Nevertheless, the

approximation error of the DC-link voltage by the CV-MPPT algorithm does not cause significant MPPT efficiency loss since the power-voltage curve of the PV array is relatively flat at low solar irradiance conditions.

V. Conclusion

In this paper, the interharmonic emission from PV inverters has been analyzed, and the mechanism of interharmonic emission at low-power operation for grid-connected PV systems has been explored. It has been observed from the frequency spectrum analysis that the perturbation from the MPPT algorithm is one of the main causes of interharmonics in the grid current, especially at the low-power operating condition. This may cause the interharmonic in the grid current due to the frequency modulation between the error in the dc-link voltage and the grid voltage. Accordingly, three mitigation solutions (i.e., adaptive gain, rate limiter and CV-MPPT methods) have been introduced in this paper to alleviate interharmonics from the PV inverters. Simulation results have been carried out on a 3-kW single-phase PV system with the mitigation solutions. It can be seen from the results that both employing an adaptive gain and a rate limiter can reduce the interharmonics significantly, which is achieved by reducing the dynamic response of the dc-link voltage controller during the MPPT perturbation period. Nevertheless, the CV-MPPT method is the most effective method among the three in terms of minimizing the interharmonics, since the perturbation in the dc-link voltage is avoided during the low-power operation. However, the MPPT accuracy is compromised, as the reference voltage at the MPP is an approximation.

Acknowledgment

References

[1] A. R. Oliva and J. C. Balda, "A PV dispersed generator: a power quality analysis within the IEEE 519," *IEEE Trans. Power Del.*, vol. 18, no. 2, pp. 525–530, Apr. 2003.

[2] F. Katiraei, K. Mauch, and L. Dignard-Bailey, "Integration of photovoltaic power systems in high-penetration clusters for distribution networks and mini-grids," *Int. J. Distrib. Energy Resources*, vol. 3, no. 3, pp. 207–223, 2007.

[3] E. Fuchs and M. A. Masoum, *Power quality in power systems and electrical machines*. New York: Academic/Elsevier, 2008.

[4] R. K. Varma, S. A. Rahman, T. Vanderheide, and M. D. N. Dang, "Harmonic impact of a 20-MW PV solar farm on a utility distribution network," *IEEE Power Energy Technol. Syst. J.*, vol. 3, no. 3, pp. 89–98, Sep. 2016.

[5] D. Gallo, R. Langella, A. Testa, J. C. Hernandez, I. Papic, B. Blazic, and J. Meyer, "Case studies on large PV plants: Harmonic distortion, unbalance and their effects," in *Proc. IEEE Power Energy Soc. General Meeting*, pp. 1–5, Jul. 2013.

[6] J. H. R. Enslin and P. J. M. Heskes, "Harmonic interaction between a large number of distributed power inverters and the distribution network," *IEEE Trans. Power Electron.*, vol. 19, no. 6, pp. 1586–1593, Nov. 2004.

[7] D. G. Infield, P. Onions, A. D. Simmons, and G. A. Smith, "Power quality from multiple grid-connected single-phase inverters," *IEEE Trans. Power Del.*, vol. 19, no. 4, pp. 1983–1989, Oct. 2004.

[8] Y. Yang, K. Zhou, and F. Blaabjerg, "Current harmonics from single-phase grid-connected inverters - examination and suppression," *IEEE J. Emerg. Sel. Top. Power Electron.*, vol. 4, no. 1, pp. 221–233, Mar. 2016.

[9] T. Messo, J. Jokipii, A. Aapro, and T. Suntio, "Time and frequency-domain evidence on power quality issues caused by grid-connected three-phase photovoltaic inverters," in *Proc. EPE*, pp. 1–9, Aug. 2014.

[10] P. Koponen, H. Hansen, and M. Bollen, "Interharmonics and light flicker," in *Proc. CIRED*, pp. 1–5, Jun. 2015.

[11] M. Aiello, A. Cataliotti, S. Favuzza, and G. Graditi, "Theoretical and experimental comparison of total harmonic distortion factors for the evaluation of harmonic and interharmonic pollution of grid-connected photovoltaic systems," *IEEE Trans. Power Del.*, vol. 21, no. 3, pp. 1390–1397, Jul. 2006.

[12] G. Chicco, J. Schlabbach, and F. Spertino, "Experimental assessment of the waveform distortion in grid-connected photovoltaic installations," *Solar Energy*, vol. 83, no. 7, pp. 1026–1039, Jul. 2009.

[13] R. Langella, A. Testa, S. Z. Djokic, J. Meyer, and M. Klatt, "On the interharmonic emission of PV inverters under different operating conditions," in *Proc. ICHQP*, pp. 733–738, Jun. 2016.

[14] R. Langella, A. Testa, J. Meyer, F. Mller, R. Stiegler, and S. Z. Djokic, "Experimental-based evaluation of PV inverter harmonic and interharmonic distortion due to different operating conditions," *IEEE Trans. Instrum. Meas.*, vol. 65, no. 10, pp. 2221–2233, Oct. 2016.

[15] P. Pakonen, A. Hilden, T. Suntio, and P. Verho, "Grid-connected PV power plant induced power quality problems - experimental evidence," in *Proc. EPE*, pp. 1–10, Sep. 2016.

[16] X. Xu, A. J. Collin, S. Djokic, S. Yanchenko, F. Moller, J. Meyer, R. Langella, and A. Testa, "Analysis and modelling of power-dependent harmonic characteristics of modern PE devices in LV networks," *IEEE Trans. Power Del.*, vol. PP, no. 99, pp. 1–9, 2016.

[17] A. Testa, M. F. Akram, R. Burch, G. Carpinelli, G. Chang, V. Dinavahi, C. Hatziadoniu, W. M. Grady, E. Gunther, M. Halpin, P. Lehn, Y. Liu, R. Langella, M. Lowenstein, A. Medina, T. Ortmeyer, S. Ranade, P. Ribeiro, N. Watson, J. Wikston, and W. Xu, "Interharmonics: Theory and modeling," *IEEE Trans. Power Del.*, vol. 22, no. 4, pp. 2335–2348, Oct. 2007.

[18] M. R. Rifai, T. H. Ortmeyer, and W. J. McQuillan, "Evaluation of current interharmonics from AC drives," *IEEE Trans. Power Del.*, vol. 15, no. 3, pp. 1094–1098, Jul. 2000.

[19] F. D. Rosa, R. Langella, A. Sollazzo, and A. Testa, "On the interharmonic components generated by adjustable speed drives," *IEEE Trans. Power Del.*, vol. 20, no. 4, pp. 2535–2543, Oct. 2005.

[20] H. Soltani, F. Blaabjerg, F. Zare, and P. C. Loh, "Effects of passive components on the input current interharmonics of adjustable-speed drives," *IEEE J. Emerg. Sel. Top. Power Electron.*, vol. 4, no. 1, pp. 152–161, Mar. 2016.

[21] L. F. Beites, J. G. Mayordomo, A. Hernandez, and R. Asensi, "Harmonics, interharmonics and unbalances of arc furnaces: a new frequency domain approach," *IEEE Trans. Power Del.*, vol. 16, no. 4, pp. 661–668, Oct. 2001.

[22] C. Vilar, J. Usaola, and H. Amaris, "A frequency domain approach to wind turbines for flicker analysis," *IEEE Trans. Energy Convers.*, vol. 18, no. 2, pp. 335–341, Jun. 2003.

[23] F. Blaabjerg, R. Teodorescu, M. Liserre, and A.V. Timbus, "Overview of control and grid synchronization for distributed power generation systems," *IEEE Trans. Ind. Electron.*, vol. 53, no. 5, pp. 1398–1409, Oct. 2006.

[24] M. Ciobotaru, "Reliable grid condition detection and control of single-phase distributed power generation systems," Ph.D. dissertation, Aalborg University, 2009.

[25] N. Femia, G. Petrone, G. Spagnuolo, and M. Vitelli, "Optimization of perturb and observe maximum power point tracking method," *IEEE Trans. Power Electron.*, vol. 20, no. 4, pp. 963–973, Jul. 2005.

[26] T. Esram and P.L. Chapman, "Comparison of photovoltaic array maximum power point tracking techniques," *IEEE Trans. Energy Convers.*, vol. 22, no. 2, pp. 439–449, Jun. 2007.

[27] C. Dorofte, U. Borup, and F. Blaabjerg, "A combined two-method MPPT control scheme for grid-connected photovoltaic systems," in *Proc. EPE*, pp. 1–10, Sep. 2005.